Proceedings of the 5th International Conference on Nonlinear Dynamics
ND-KhPI2016
September 27-30, 2016, Kharkov, Ukraine

R-functions in Development of Analytical Identification of Geometrical Objects

Tetyana I. Sheiko[1*], Yulia S. Litvinova[1], Kyrylo V. Maksymenko-Sheiko[1,2]

Abstract
In this paper for mathematical and computer modeling of fractal geometry objects, machine parts and building structure the R-functions theory is applied The mathematical tools of the R-functions theory are very convenient for the fractal geometry objects description. The equations of the Levi fractal, Pythagoras's tree, Koch's curve, cross and snowflake, Menger's sponge (also known as the Menger universal curve), Sierpinski's carpet, etc. have been constructed. The techniques using both the equations of three-dimensional primitives, and information about the equations of boundaries of sections of reset object have been developed The equations of the automobile body surface, the bearing sleeve, the stepped shaft having two cogged pulleys, the rotary valve, the revolver drum, the screw having the shaped head, cut and lock surface, the cutter lift, the oil filter arm, etc. were constructed. The equations of the hexahedral cartridge having 91 fuel elements have been constructed using only two R-operations.

Keywords
R-functions, 3D-printing, fractal geometry, machine-building details, building structures

[1] Podgorny Institute for Mechanical Engineering Problems of NAS of Ukraine, Kharkov, Ukraine
[2] Karazin Kharkov National University, Kharkov, Ukraine
*** Corresponding author:** sheyko@ipmach.kharkov.ua

Introduction

In 1637 Descartes in his work "Geometry" formulated the inverse problem of analytical geometry: "to describe defined geometrical object by equation". In 1963 (after 326 years) academician Rvachev V. L. created the R-functions theory and solved this problem. V. L. Rvachev used methods of logic algebra and systems of elementary continuous functions of the real arguments. These functions are similar to functions of logic algebra because the function sign is uniquely defined by signs of its arguments. From 1963 till 2005 a large number of equations of geometrical objects have been constructed by Rvachev V. L. and his disciples. In the last decade, considerable attention was paid to the development of the methods to automate this process, to reduce the number of R-operations taking into account symmetry of the boundary. It allowed to expand significantly the possibilities of analytical identification of geometrical objects. The mathematical tools of the R-functions theory are very convenient for the fractal geometry objects description. The equations of the Levi fractal, Pythagoras's tree, Koch's curve, cross and snowflake, Menger's sponge (also known as the Menger universal curve), Sierpinski's carpet, etc. were constructed. In recent years special attention was paid to creation of the equations of machine-building details in 3D. At the same time techniques using both the equations of three-dimensional primitives, and information about the equations of boundaries of sections of reset object were developed. The equations of the automobile body surface, the bearing sleeve, the stepped shaft having two cogged pulleys, the rotary valve, the revolver drum, the screw having the shaped head, cut and lock surface, the cutter lift, the oil filter arm, etc. were constructed. The equation of the hexahedral cartridge having 91 fuel elements has been constructed using only two R-operations. This paper gives the examples of mathematical models of some of these geometrical objects.

1. Mathematical models of the fractal geometry objects.

Let's write the equation of Menger's sponge which is three-dimensional analogue of Sierpinski's carpet:

$\omega_0(x,y,z)=\dfrac{a^2-x^2}{2a}\wedge_0\dfrac{a^2-y^2}{2a}\wedge_0\dfrac{a^2-z^2}{2a}\geq 0$ is the equation of cube with a side $2a$.

$\omega b_1=\dfrac{1}{3}\left(\dfrac{a^2-9x^2}{2a}\wedge_0\dfrac{a^2-9y^2}{2a}\right)\vee_0\left(\dfrac{a^2-9z^2}{2a}\wedge_0\dfrac{a^2-9x^2}{2a}\right)\vee_0\left(\dfrac{a^2-9z^2}{2a}\wedge_0\dfrac{a^2-9y^2}{2a}\right)\geq 0$ is the equation of three central through holes.

$$\omega b_k=\frac{1}{3^k}\left(\frac{a^2-3^{2k}\mu_{xk}{}^2}{2a}\wedge_0\frac{a^2-3^{2k}\mu_{yk}{}^2}{2a}\right)\vee_0\left(\frac{a^2-3^{2k}\mu_{zk}{}^2}{2a}\wedge_0\frac{a^2-3^{2k}\mu_{xk}{}^2}{2a}\right)\vee_0$$

$$\vee_0\left(\frac{a^2-3^{2k}\mu_{zk}{}^2}{2a}\wedge_0\frac{a^2-3^{2k}\mu_{yk}{}^2}{2a}\right)\geq 0,\quad (k=2,3,...)$$ — the equations of translated self-similar holes where $\mu_{xk}=\dfrac{h_k}{\pi}\arcsin\sin\dfrac{\pi x}{h_k};\mu_{yk}=\dfrac{h_k}{\pi}\arcsin\sin\dfrac{\pi y}{h_k};\mu_{zk}=\dfrac{h_k}{\pi}\arcsin\sin\dfrac{\pi z}{h_k};\ h_k=\dfrac{2a}{3^{k-1}};$

$\omega_k=\omega_0\wedge_0\omega b_1\wedge_0\omega b_2\wedge_0\ldots\wedge_0\omega b_k\geq 0$.

In fig. 1 a visualization of the equation of Menger's sponge surface is shown.

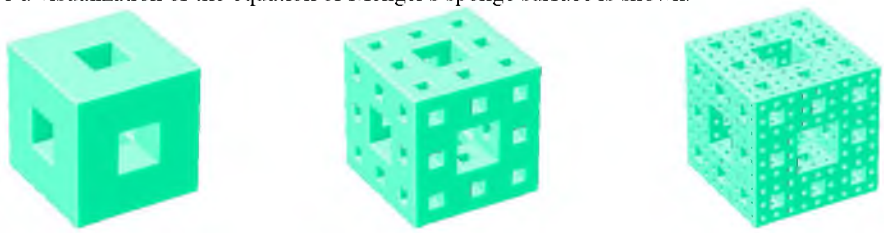

$k=1$ $k=2$ $k=3$

Figure 1. Menger's sponge

Let's consider the Levi fractal. For construction an isosceles right triangle is taken, and then each leg is replaced with a similar triangle. So

$\omega_1(x,y)=y\wedge_0((x-y+3a)\wedge_0(-x-y+3a))\geq 0;\ \omega_{k1}(x,y)=\omega_{k-1}(x+y+1.5a,\ -x+y-1.5a)\geq 0$

$\omega_{k2}(x,y)=\omega_{k1}(-x,y)\geq 0;\ \omega_k(x,y)=\omega_{k1}(x,y)\vee_0\omega_{k2}(x,y)\geq 0\ \ (k=2,3,4,....)$

The figure 2 shows a picture of the level curves of constructed equation.

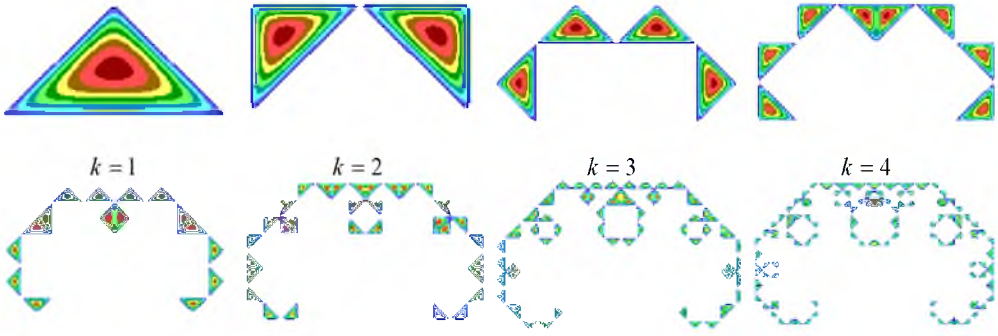

$k=1$ $k=2$ $k=3$ $k=4$

$k=5$ $k=6$ $k=7$ $k=8$

Figure 2. The Levi fractal

When Pythagoras proved his famous theorem, he built a shape where squares are located at the sides of a right triangle. Nowadays, this figure has increased in the whole Pythagoras tree. One of the characteristics is the following. If the area of the first square is equal to 1, then the sum of the areas of the squares will also be 1 at each level. So

$\omega_0=\dfrac{a^2-x^2}{2a}\wedge_0\dfrac{a^2-y^2}{2a}\geq 0,\ \omega p_1=\dfrac{0{,}5a^2-x_1^2}{a\sqrt{2}}\wedge_0\dfrac{0{,}5a^2-y_1^2}{a\sqrt{2}}\geq 0,\ \omega l_1(x,y)=\omega p_1(-x,y)\geq 0.$

$x_1 = \frac{\sqrt{2}}{2}((x-a)+(y-2a)),\ y_1 = \frac{\sqrt{2}}{2}(-(x-a)+(y-2a)).\ \omega_1(x,y) = \omega_0 \vee_0 (\omega p_1 \vee_0 \omega l_1) \geq 0$

$\omega_{k-1,1}(x,y) = \omega_{k-1}(2(x-1.5a),2(y-3.5a)) \geq 0.$

$\omega_{k-1,2}(x,y) = \omega_{k-1}(-2(y-2a-a/2),2(x-2a-a/2)) \geq 0.$

$\omega p_k(x,y) = \frac{\omega_{k-1,1}(x,y)}{2^{k-1}} \vee_0 \frac{\omega_{k-1,2}(x,y)}{2^{k-1}} \geq 0,\ \omega l_k(x,y) = \omega p_k(-x,y) \geq 0,$

$\omega_k(x,y) = \omega_{k-1} \vee_0 (\omega p_k \vee_0 \omega l_k) \geq 0 \qquad k = 2,3,....$

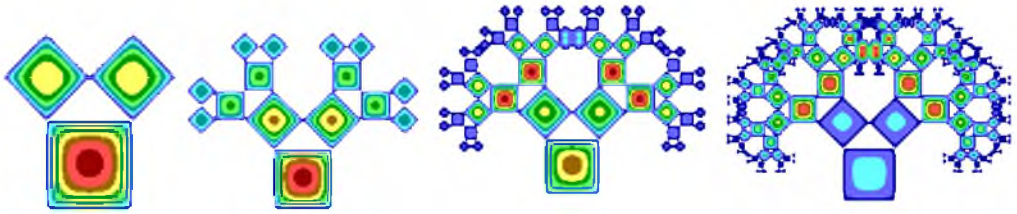

$k=1$ $k=2$ $k=3$ $k=4$

Figure 3. Pythagoras's tree

The R-functions method allows to receive easily reoriented Koch's curve, having taken the negation of the Koch's curve function [5] (fig.4, 5).

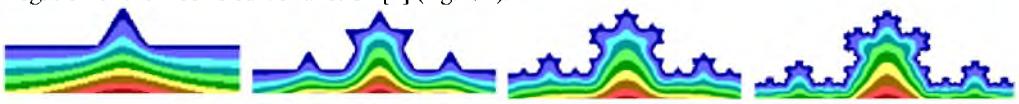

$k=1$ $k=2$ $k=3$ $k=4$

Figure 4. Koch's curve

$k=1$ $k=2$ $k=3$ $k=4$

Figure 5. Reoriented Koch's curve

Now it is possible to build the equation of Koch's cross (fig.6), carrying out the following transformations $\omega K_k = \omega_k(r\sin\mu,\ r\cos\mu - R) \geq 0,\ \mu(n0) = \frac{2}{n}\arcsin\left(\sin\frac{n\theta}{2}\right)$, R is the radius of the circle which is inscribed in the right p-gon with a side equal to the interval at which the Koch's curve was constructed.

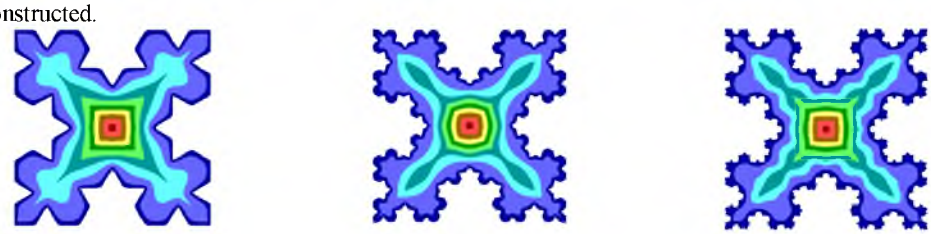

$k=2$ $k=3$ $k=4$

Figure 6. Koch's cross on the square sides

2. Mathematical model of the fuel cartridge with 91 fuel elements.

Let's construct the equation of the fuel cartridge:

$\sigma \equiv R_v - x$, $\mu_v = \frac{4}{3\pi}\sum_k (-1)^{k+1} \frac{\sin[(2k-1)3\theta]}{(2k-1)^2}$, $r = \sqrt{x^2 + y^2}$. $\omega_b \equiv R_v - r\cos\mu_v = 0$ is the equation of hexahedral casing of the cartridge.

Let's consider the extended triangular packaging.

$f_1 = R^2 - \mu_x^2 - \mu_y^2 \geq 0$,

$$\mu_x = \frac{4h_x}{\pi^2}\sum_k (-1)^{k+1} \frac{\sin\left[(2k-1)\frac{\pi x}{h_x}\right]}{(2k-1)^2}, \quad \mu_y = \frac{4h_y}{\pi^2}\sum_k (-1)^{k+1} \frac{\sin\left[(2k-1)\frac{\pi x}{h_y}\right]}{(2k-1)^2},$$

$f_2 = R^2 - \mu_{x1}^2 - \mu_{y1}^2 \geq 0$,

$$\mu_{x1} = \frac{4h_x}{\pi^2}\sum_k (-1)^{k+1} \frac{\sin\left[\frac{(2k-1)\pi(x - h_x/2)}{h_x}\right]}{(2k-1)^2}, \quad \mu_{y1} = \frac{4h_y}{\pi^2}\sum_k (-1)^{k+1} \frac{\sin\left[\frac{(2k-1)\pi(y - h_y/2)}{h_x}\right]}{(2k-1)^2}.$$

$\omega_{tv} \equiv (f_1 \vee_0 f_2) = 0$, $\omega \equiv \omega_b \wedge_0 \overline{\omega_{tv}} = 0$.

In fig.7 the pattern of level lines of the function and the cartridge in 3D are shown. It should be noted that R-operation has been used only twice when constructing the cassette equation.

Let's consider packaging with cyclic symmetry.

$$\omega_o \equiv \frac{1}{2R_{tv}}\left(R_{tv}^2 - (x-R)^2 - y^2\right), \quad \mu_d = \frac{8}{n_d\pi}\sum_k (-1)^{k+1} \frac{\sin\left[(2k-1)\frac{n_d\theta}{2}\right]}{(2k-1)^2}.$$

$$\omega_{tv1} \equiv \frac{1}{2R_{tv}}\left(R_{tv}^2 - (r\cos\mu_d - R)^2 - (r\sin\mu_d)^2\right) = 0.$$

$$\omega_{o1} \equiv \frac{1}{2R_{tv}}\left(R_{tv}^2 - (x-R_1)^2 - y^2\right), \quad \mu_b = \frac{8}{n_b\pi}\sum_k (-1)^{k+1} \frac{\sin\left[(2k-1)\frac{n_b\theta}{2}\right]}{(2k-1)^2}.$$

$$\omega_{tv2} \equiv \frac{1}{2R_{tv}}\left(R_{tv}^2 - (r\cos\mu_b - R_1)^2 - (r\sin\mu_b)^2\right) = 0.$$

$$\omega_{o2} \equiv \frac{1}{2R_{tv}}\left(R_{tv}^2 - (x-R_2)^2 - y^2\right), \quad \mu_c = \frac{8}{n_c\pi}\sum_k (-1)^{k+1} \frac{\sin\left[(2k-1)\frac{n_c\theta}{2}\right]}{(2k-1)^2}.$$

$$\omega_{tv3} \equiv \frac{1}{2R_{tv}}\left(R_{tv}^2 - (r\cos\mu_c - R_2)^2 - (r\sin\mu_c)^2\right) = 0. \quad \omega \equiv \left(\omega_b \wedge_0 \overline{\omega_{tv1} \vee_0 \omega_{tv2} \vee_0 \omega_{tv3}}\right) \geq 0.$$

So, the equation of the cartridge border with 91 fuel elements is the seven-parameter $(n_b, n_d, n_c, R, R_1, R_2 R_{tv})$ curves family (fig.7). It should be noted that the R-operation was used only three times. When there is a central fuel element we receive

$$\omega \equiv \omega_b \wedge_0 \overline{\omega_{tv1} \vee_0 \omega_{tv2} \vee_0 \omega_{tv3} \vee_0 \frac{1}{2R_{tv}}\left(R_{tv}^2 - x^2 - y^2\right)} \geq 0.$$

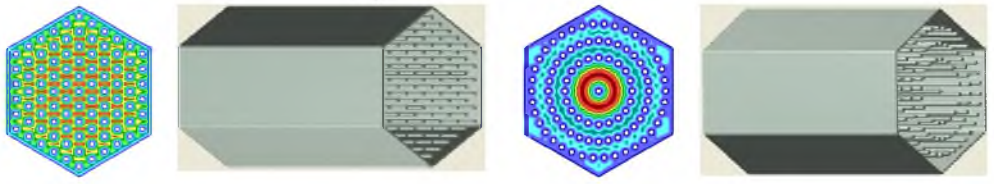

Figure 7. Fuel cartridge with 91 fuel elements, located at a chess packaging and at translation with cyclic symmetry

3. Mathematical model of the car suspension sleeve.

Let's present the equation of the car suspension sleeve:

$f1 = ((((3^2 - x^2) \wedge_0 (-5{,}5 - z)) \vee_0 (2{,}5^2 - x^2)) \wedge_0 (5^2 - y^2) \wedge_0 (6{,}5 + z)(-2{,}5 - z)) \geq 0$.

$f2 = ((-z + \frac{y}{1{,}5}) \wedge_0 (-z - \frac{y}{1{,}5})) \wedge_0 f1 \geq 0$ is the lower platform of a sleeve with a beveled edge (Fig. 8a)

$f3 = ((2{,}5^2 - y^2 - (z+2)^2) \vee_0 f2) \wedge_0 (4^2 - x^2) \geq 0$ is the platform of a sleeve connected to the cylinder (Fig. 8b)

$f4 = ((-1{,}3)^2 + y^2 + (z+2)^2 \wedge_0 f3) \geq 0$ the hole in the cylinder of sleeve is added (Fig. 8c)

$f5 = (1{,}5^2 - x^2) \wedge_0 (4{,}5 - y)(-2 + y) \geq 0$,

$f6 = (1{,}5^2 - x^2) \wedge_0 (4{,}5 + y)(-2 - y) \geq 0$, $f7 = (f5 \vee_0 f6) \wedge_0 (5{,}5 + z) \geq 0$ are the sides depressions (Fig. 8d). $W_{sleeve} = f4 \wedge_0 (-f7) \geq 0$.

The step-by-step visualization of the built sleeve equation in 3D is shown in fig.8.

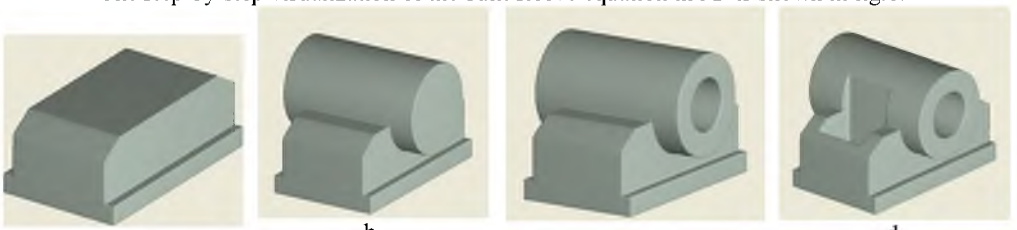

a b c d

Figure 8. The car suspension sleeve

4. Mathematical model of oil filter bracket.

Bellow the equation of the filter bracket is presented:

$$f1 = \left(1 - \left(\frac{x}{5{,}8}\right)^2 - \left(\frac{y}{5{,}8}\right)^2 - \frac{(z+0{,}3)^2}{1{,}6^2}\right) \wedge_0 (5{,}7^2 - x^2 - y^2) \geq 0,$$

$$f2 = ((4{,}5^2 - x^2) \wedge_0 (4{,}5^2 - y^2) \wedge_0 (6{,}1^2 - x^2 - y^2) \vee_0 f1) \wedge_0 (1 - z^2) \geq 0$$

$$fs = (0{,}8^2 - y^2 - (z - 0{,}1)^2) \wedge_0 ((5{,}8 - x)(x - 4{,}5)) \geq 0,$$

$$fss = (0{,}4^2 - y^2 - (z - 0{,}1)^2) \wedge_0 ((5{,}8 - x)(x - 4{,}5)) \geq 0, \quad f3 = (f2 \vee_0 fs) \wedge_0 (-fss) \geq 0, \text{ (Fig.9a)}$$

$$f44 = ((4{,}5^2 - x^2 - y^2 - z^2) \wedge_0 (-z)) \wedge_0 (x^2 + y^2 + z^2 - 3{,}5^2) \geq 0.$$

$$flen = 1 - \left(\frac{x}{4{,}6}\right)^2 - \left(\frac{y}{4{,}6}\right)^2 - \frac{(z+0{,}3)^2}{1{,}1^2}. \quad f4 = (f3 \vee_0 f44) \wedge_0 (-flen) \geq 0. \text{ (Fig.9b)}$$

n_o=4, $r_o = \sqrt{x^2 + y^2}$, $\theta = arctg\frac{y}{x}$, $ff2 = \left(\theta - \frac{\pi}{4}\right)\frac{n_o}{2}$, $\mu_2 = \frac{8}{n_o \pi}\sum_k (-1)^{k+1}\frac{\sin[(2k-1)ff2]}{(2k-1)^2}$,

$x_2 = r_o \cos(\mu_2)$, $y_2 = r_o \sin(\mu_2)$. $fbd = (-(x_2 - 5)^2 - y_2^2 + 0{,}3^2) \wedge_0 (z + 1{,}2) \geq 0$.

$ft = ((1{,}5^2 - (r_o - 3{,}5)^2 - (z + 4{,}5)^2) \wedge_0 (z + 5) \wedge_0 (4{,}3 - x)) \geq 0$.

n_{o1}=10, $ff = \theta\frac{n_{o1}}{2}$, $\mu = \frac{8}{n_{o1}\pi}\sum_k (-1)^{k+1}\frac{\sin[(2k-1)ff]}{(2k-1)^2}$, $x_1 = r_o \cos(\mu)$, $y_1 = r_o \sin(\mu)$.

$fnd1 = (0{,}45^2 - (z + 3{,}9)^2 - y_1^2) \wedge_0 (5{,}2 - x_1)(x_1 - 3)$,

$fnd2 = (0{,}25^2 - (z + 3{,}9)^2 - y_1^2) \wedge_0 (5{,}2 - x_1)(x_1 - 3)$. $f55 = (ft \vee_0 fnd1) \wedge_0 (-fnd2) \geq 0$.

$fnis = \left(0{,}65^2 - (z+3{,}9)^2 - y^2\right) \wedge_0 x - 3 \geq 0$, $f5 = \left(\left(f4 \vee_0 f55\right) \wedge_0 (-fbd) \wedge_0 (-fnis)\right) \geq 0$ (Fig.9c)

$fil1 = \left(\left(5{,}5^2 - x^2 - y^2\right) \wedge_0 \left((z+5)(-z-4{,}3)\right) \wedge_0 (4{,}3-x)\right) \vee_0 f5 \geq 0$,

$f6 = \left(\left(1{,}4^2 - x^2 - y^2\right) \wedge_0 \left(x^2 + y^2 - 0{,}7^2\right)\right) \wedge_0 (0{,}1-z)(z+4) \geq 0$, $fil = \left(fil1 \vee_0 f6\right) \geq 0$.

$fs1 = \left(1{,}8^2 - y^2\right) \wedge_0 \left((-z-3)(4{,}2+z)\right) \wedge_0 \left((x-3)(4{,}3-x)\right) \geq 0$,

$fs2 = \left(1{,}5^2 - y^2\right) \wedge_0 \left((-z-3)(4{,}2+z)\right) \wedge_0 (4{,}3-x) \geq 0$.

$ffi = \left((fil \vee_0 fs1) \wedge_0 (-fnis) \wedge_0 (-fs2)\right) \geq 0$ (Fig.9d).

$h = 0{,}2$, $f = arctg\dfrac{y}{x}$, $xx = \sqrt{x^2+y^2}$, $zz = z - \dfrac{h \cdot f}{2\pi}$, $ff = \pi\dfrac{zz}{h}$, $\mu = \dfrac{4h}{\pi^2}\sum_{i=1}^{\infty}(-1)^{i+1}\dfrac{\sin((2i-1)ff)}{(2i-1)^2}$,

$ff3 = \left(0{,}2^2 - (xx-0{,}7)^2 - \mu^2\right) \wedge_0 (z+4) \geq 0$.

$f_m = arctg\dfrac{z}{y}$, $yy_m = \sqrt{(z+3{,}9)^2 + y^2}$, $xx_m = x - \dfrac{h \cdot f_m}{2\pi}$, $ff_m = \dfrac{\pi \cdot xx_m}{h}$,

$\mu_m = \dfrac{4h}{\pi^2}\sum_{i=1}^{\infty}(-1)^{i+1}\dfrac{\sin((2i-1)ff_m)}{(2i-1)^2}$, $ff3_m = \left(0{,}2^2 - (yy_m - 0{,}65)^2 - \mu^2\right) \wedge_0 (x-2)(4{,}1-x) \geq 0$ —

thread cutting. $W(x,y,z) = \left(ffi \wedge_0 (-ff3)\right) \wedge_0 (-ff3_m) \geq 0$.

In Fig.9. the visualization of phased construction is shown.

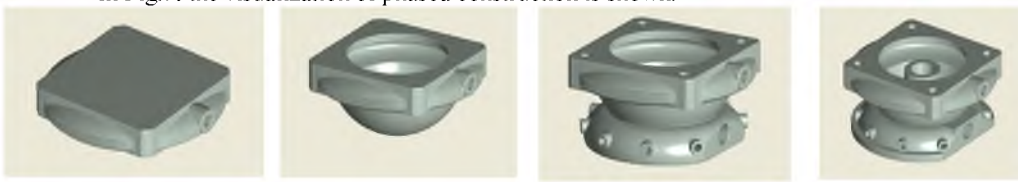

a b c d

Figure 9. The oil filter bracket

5. Mathematical model of the ship body.

The equation was constructed using information about the equations of the boundaries of cross-sections of the restored object. Vladimir Logvinovich dreamed about it. Below is the corresponding program in the "RFPreview" system language.

```
h0=-4;h1=-3;h2=2;h3=4;h4=6;h5=9;h6=11;h7=12;
a1=0.8;a2=0.65;a3=0.8;a4=1.2;a5=2;a6=5;pi=3.1415;
f1=z-a1*y^2;
x1=(x-h0)/(h1-h0);x2=(x-h2)/(h1-h2);
xx1=(x1+x2-abs(x1-x2))*0.5;w1=(xx1+abs(xx1))*0.5;
f2=z-a2*y^2;
x3=(x-h1)/(h2-h1);x4=(x-h3)/(h2-h3);
xx2=(x3+x4-abs(x3-x4))*0.5;w2=(xx2+abs(xx2))*0.5;
f3=z-a3*y^2;
x5=(x-h2)/(h3-h2);x6=(x-h4)/(h3-h4);
xx3=(x5+x6-abs(x5-x6))*0.5;w3=(xx3+abs(xx3))*0.5;
f4=z-a4*y^2;
x7=(x-h3)/(h4-h3);x8=(x-h5)/(h4-h5);
xx4=(x7+x8-abs(x7-x8))*0.5;w4=(xx4+abs(xx4))*0.5;
f5=z-a5*y^2;
x9=(x-h4)/(h5-h4);x10=(x-h6)/(h5-h6);
xx5=(x9+x10-abs(x9-x10))*0.5;w5=(xx5+abs(xx5))*0.5;
f6=z-a6*y^2;
x11=(x-h5)/(h6-h5);x12=(x-h7)/(h6-h7);
xx6=(x11+x12-abs(x11-x12))*0.5;w6=(xx6+abs(xx6))*0.5;
ww1=(f1*w1+f2*w2+f3*w3+f4*w4+f5*w5+f6*w6);
```

```
x1=x*cos(-pi/7)+z*sin(-pi/7);
ww2=rfAND((-x1+2*y+8),(-x1-2*y+8));
ww3=rfAND(rfAND(ww1,ww2),x+3);
ww=0.3-abs(ww3);
fx=(x+3);
fz=-(z-2)+0.006*(x+3)^2;
res=rfAND(rfAND(ww,fx),fz);
```

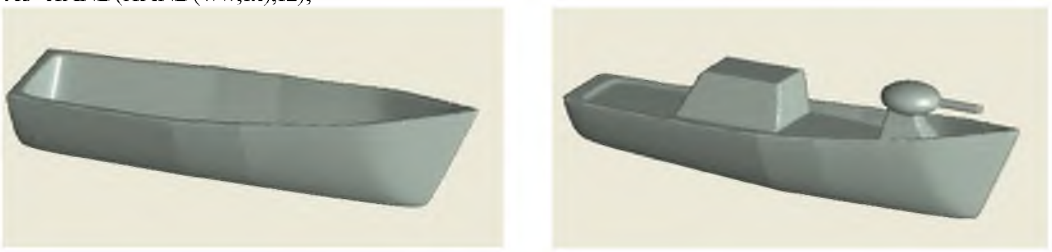

Figure 10. The surface of the ship body

6. Models of the building structures.

Currently, the 3D-printers using is very promising to create a three-dimensional physical objects. The mathematical and computer models of cottage and holiday homes with a versatile roof, with different layout, design of facades and French window were created with the help of the R-functions theory (fig. 11).

Figure 11. Cottage houses

Also the equations of various variants of home front wall designed in Amsterdam for 3D-printing were constructed (fig. 12).

Figure 12. An exterior wall of the house

Conclusions

The R-functions theory is applied for mathematical and computer modeling of fractal geometry objects, machine parts and building structures. The analytical description of designed objects makes it possible. Using the alphanumeric options allows to change the projected objects quickly, if it is necessary. The property of positivity of built functions in the interior points of the object is very convenient for the 3D printing realization.

References

[1] Rvachev V.L. *R-functions theory and some its applications*. Kiev: Nauk. dumka; 1982. In Russian.

[2] Maksymenko-Sheiko K.V. *R-functions at mathematical modeling of geometrical objects and physical fields*. Kharkov: IPMash of NAS of Ukraine; 2009. In Russian.

[3] Mandelbrot B. *Fractal geometry of nature*. Moscow: Institute for Computer Investigations; 2002. In Russian.

[4] Lisin D.O. Computer program "System of visualization and mesh building at the surface of geometric objects descripted with the help of mathematical tools of R-functions theory "RFPreview"": inventor's certificate no. 45951; 2012.

[5] Maksymenko-Sheiko K.V., Sheiko T.I. Mathematical modeling of geometric fractals using R-functions. *Cybernetics and Systems Analysis*, 2012. vol. 48, Issue 4, p. 614-620.